JOURNAL OF APPLIED ELECTROCHEMISTRY 23 (1993) 241–246

Advanced laboratory electrolyser for production of pure hydrogen

F. P. DOUSEK, K. MICKA

J. Heyrovský Institute of Physical Chemistry and Electrochemistry, Czechoslovak Academy of Sciences, 182 23 Prague 8, Czechoslovakia

Received 11 May 1992; revised 29 August 1992

A laboratory scale diaphragmless water electrolyser has been developed for the production of pure hydrogen at a pressure of up to 140 kPa by electrolysis of a KOH solution. Porous electrodes with a nickel catalyst and a copper cover layer serve as cathodes, and nickel sheets as anodes. Modular construction of the electrolyser permits simple combination of its cells into larger units. Thus, up to 20 cells with disc-shaped electrodes of 7 cm in diameter were connected in series and provided with electrolyte manifolds and automatic pressure and electrolyte level control devices. The dimensions of the electrolyte manifolds were optimized on the basis of calculations of parasitic currents. A good agreement between the calculated and measured current efficiencies was found at various cell numbers and total currents.

1. Introduction

A source of pure hydrogen, completely free of oxygen, is often needed in electrochemical, analytical, and other laboratories to remove oxygen from the analysed solutions, as a reducing agent in laboratory ovens, in gas chromatography, and other applications. Electrolytic hydrogen in pressure bottles contains about 0.2% oxygen, traces of hydrocarbons (lubricating oil used in compressors), and atmospheric gases; moreover, a drawback in using pressure bottles consists in their relatively difficult handling and safety precautions.

These difficulties can be eliminated by using a laboratory water electrolyser for production of compressed hydrogen, supplying only the amount of hydrogen needed at a given instant and close to the consuming apparatus. Home-made water electrolysers usually suffer from various imperfections and they provide impure hydrogen at a pressure of, at most, several decimetres of water. As far as the authors are aware, the hitherto known water electrolysers employ diaphragms to separate the anodic and cathodic compartments. There are several patents, however, which do not include the construction details [1–4]. Apparently, the best apparatus of this kind was constructed by Baolian and Guangya [5] using an asbestos membrane and nickel gauze electrodes; they obtained very pure hydrogen by applying absorbers of oxygen and water vapour. An electrolyser for somewhat higher hydrogen output ($1.4\,m^3\,h^{-1}$) at a pressure of up to 15 atm (~ 1.5 MPa) with porous nickel electrodes was built by Ragunathan *et al.* [6]. Divíšek *et al.* [7,8] constructed a 10 kW water electrolyser employing NiO diaphragms and Raney nickel electrodes for production of hydrogen of technical purity at atmospheric pressure. The alkaline water electrolyser built by Vandenborre *et al.* [9] contains a Co spinel and NiS deposited on perforated nickel sheets as anode and cathode, respectively, and an inorganic ion-exchange membrane in between; up to 60 cells are combined in a filter-press arrangement, with an electrode area up to $0.2\,m^2$, and operating voltage at 1.6 V per cell at 90° C and $2000\,A\,m^{-2}$ or 1.9 V at $10^4\,A\,m^{-2}$. The hydrogen overpressure is in the range of 0.5–4 atm (50–400 kPa).

Commercial pressure electrolysers (e.g. H_2/O_2 gas generator HG 1000 C, Teledyne Energy Systems, USA) usually have rather high outputs and must be combined with an apparatus ensuring reliable proportional consumption of both gases, even when only hydrogen is required. Breakdown of the equipment can lead to the formation of compressed explosive mixtures.

During investigations of H_2/O_2 fuel cells performed at this Institute in the 1960s, considerable experience was obtained in preparing porous nickel electrodes with a Raney nickel catalyst for hydrogen of the DSK type according to Justi and Winsel [10,11], which were later used in constructing a hydrogen generator [12,13]. This was gradually made fully automatic and equipped with an electrolyte level control device [14]; a small unit of six disc-shaped electrodes, 3.1 cm (diam.), connected in parallel, yielded (at $80\,mA\,cm^{-2}$) $2\,dm^3$ of pure hydrogen per hour at an overpressure of up to 100 kPa, while oxygen produced at atmospheric pressure was vented into the atmosphere. After many years experience, an enlarged version of this water electrolyser was developed, and this is described below.

2. Description of the apparatus

The principal part of the electrolyser is the disc-shaped, porous metal electrode shown schematically in Fig. 1. The electrode is provided with 0.7 mm thick, finely porous copper cover layers on both sides (3),

0021-891X

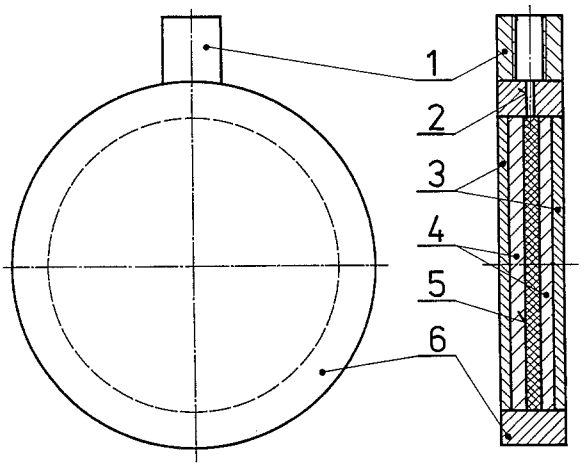

Fig. 1. Scheme of the porous metal electrode for evolution of hydrogen under pressure. (1) nut, (2) outlet opening in the circumferential ring, (3) finely porous Cu cover layer, (4) catalytic Ni layer, (5) central Ni layer with coarse pores, and (6) circumferential Cu ring.

containing 35 vol % of pores with radii below 1 μm. The cover layers are made by moulding electrolytic copper powder, whose particles have a dendritic structure, at a pressure of 100 MPa. The circumferential ring of 7 cm diameter (6) is made from the same material. The 1.3 mm thick catalytic layers (4) consist of a porous nickel skeleton supporting a Raney nickel catalyst [15,16]. Hydrogen is evolved electrolytically on this material in 3.5 M KOH at a low overpotential, even at higher current densities, as can be seen from curve (a) in Fig. 2 (the potential of the reversible hydrogen electrode in the same medium is -930 mV against Hg/HgO).

The catalytic layers (1.3 mm thick, 6.2 cm diam., 75% porosity) contain two superimposed pore systems: a coarse one, formed by thermal decomposition of a filler ($(NH_4)_2C_2O_4 \cdot H_2O$) during sintering the whole electrode at 450 °C in hydrogen atmosphere [17], and a fine one, formed by intergranular spaces. The KOH solution is expelled from the larger pores by a hydrogen overpressure of less than 10 kPa, while the smaller pores remain drowned up to an overpressure of about 130 kPa, similarly to the pores in the cover layers. Thus, ionic conduction is ensured for reduction of water to hydrogen.

The hydrogen evolved in the catalytic layers escapes through the gas-filled pores into the 1 mm thick middle layer, (5) in Fig. 1, of sintered nickel with large (0.2–0.4 mm) pores, forming 50% of its volume. The gas passes easily through this layer and then through the outlet hole (2) into the gas conduit. The hydrogen leaving the electrolyser contains less than 0.01 mg of KOH per dm^3 even at full output. Such a high purity is due to the fact that the evolved hydrogen, instead of forming bubbles, diffuses from the three-phase interface directly into the gas-filled pores.

The polarization curve of the complete electrode (Fig. 2b) is shifted to more negative potentials compared to that of the operating layer alone (curve a) as a result of the ohmic potential drop and resistance against diffusion in the cover layers. Nevertheless, it can be seen from Fig. 2 that the hydrogen evolution takes place only in the catalytic layers if the current density is not too high (compare curve b with c).

After some time of operation, any residues of air are expelled from the gas space and the electrolyte in the cell becomes saturated with oxygen evolving at the anode (a nickel sheet). Although some oxygen may diffuse through the cover layer into the operating layer, it is rapidly reduced electrochemically to OH^- ions. Thus, no detectable quantity of oxygen can be found in the hydrogen leaving the electrolyser.

If, for any reason, the overpressure of hydrogen exceeds the capillary pressure in the cover layers, then the gas passes through their pores into the bulk electrolyte and finally into the atmosphere. Thus, the electrode acts as a safety valve. As soon as the overpressure of hydrogen is decreased, the cover layer pores are drowned again.

The electrolyser can be built up by assembling a suitable number of modules, as shown schematically in Fig. 3 (with a nominal output of 2 dm^3 of H_2 per cell at 5 A). Each module contains two short-circuited circular nickel sheets as positive electrodes with one catalytic porous electrode in between. All cells are connected in series, hence the current need not be too large in proportion to the applied voltage and the electrolyte space is made relatively small. The electrolyte (3.5 M KOH) is recirculated through the channels, portions of which are depicted in the drawing. The circulation is effected by the gas lift action of oxygen bubbles. The electrolyte manifold is connected with a reservoir, in which the electrolyte level is electronically controlled and pure water is automatically added if necessary.

The dimensions of the electrolyte conduits must be chosen to keep the parasitic currents flowing through them as small as possible, while also keeping the hydrodynamic resistance as low as possible. These two requirements are, of course, opposed and therefore it was necessary first to develop a theory permitting the calculation of the parasitic currents, and thus, also, the current efficiency of the electrolyser.

3. Calculation of parasitic currents

For the calculation of parasitic currents, the electrolyser described in the previous Section can be modelled by the equivalent circuit shown in Fig. 4 [18,19]; the resistances are denoted by subscripts corresponding to the channels in Fig. 3. The electrolyser is divided into $m = N - 1$ sections, where N is the number of cells, as shown by the dashed lines in Fig. 3, each section (i.e. a fictitious cell) including an anode, short circuited with a cathode, and an insulating wall between them. These fictitious cells are represented by the resistances R_1 to R_m in Fig. 4 (the Nth fictitious cell, consisting of the first and of the final electrode, is represented by R_0).

In further considerations, the branches of the equivalent circuit are numbered as in Fig. 4; these numbers

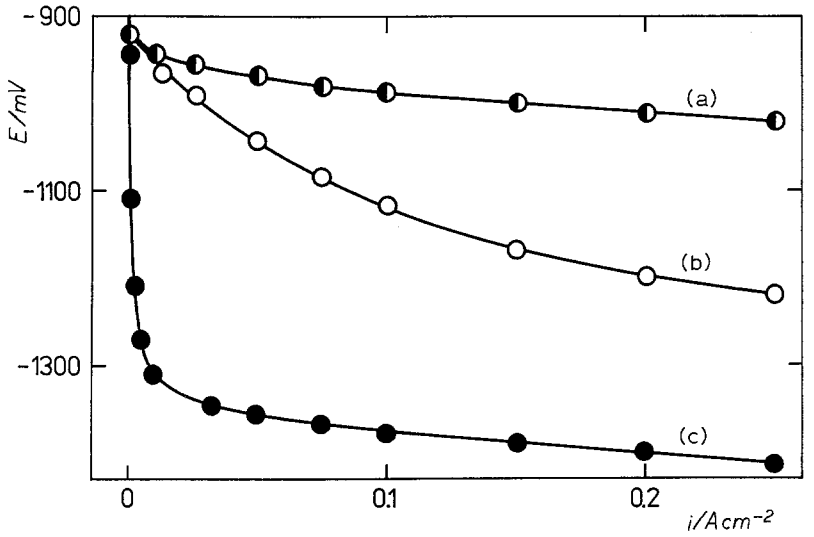

Fig. 2. Dependence of the potential, E (in mV against Hg/HgO) on the current density, i (A cm^{-2} of geometric surface area of cover layer). (a) Catalytic Ni layer; (b) electrode according to Fig. 1; (c) Cu cover layer. Electrolyte 3.5 M KOH at 25 °C.

are used as subscripts to denote the particular currents. The current I_1 flowing through the branch 1 with the fictitious cell resistance R_1 produces a voltage drop:

$$I_1 R_1 = A_c + B_c I_1 \quad (1)$$

which is equal to the potential difference between the electrolyte at the anode and at the cathode of the fictitious cell 1. Analogously, the current I_6 flowing through the branch 6 with resistance R_2 produces a voltage drop:

$$I_6 R_2 = A_c + B_c I_6 \quad (2)$$

and so on. Now, by applying Kirchhoff's laws to the circuit in Fig. 4, a system of linear equations for all the particular currents is obtained. For example, the first five equations are as follows:

$$A_c + B_c I_1 - I_2 R_{1D} - I_2 R_{2D} + I_4 R_{1D} = 0 \quad (3)$$

$$A_c + B_c I_1 - I_3 R_{1H} - I_3 R_{2H} + I_5 R_{1H} = 0 \quad (4)$$

$$I_2 + I_4 - I_7 = 0 \quad (5)$$

$$I_1 - I_4 - I_5 - I_6 = 0 \quad (6)$$

$$I_3 + I_5 - I_8 = 0 \quad (7)$$

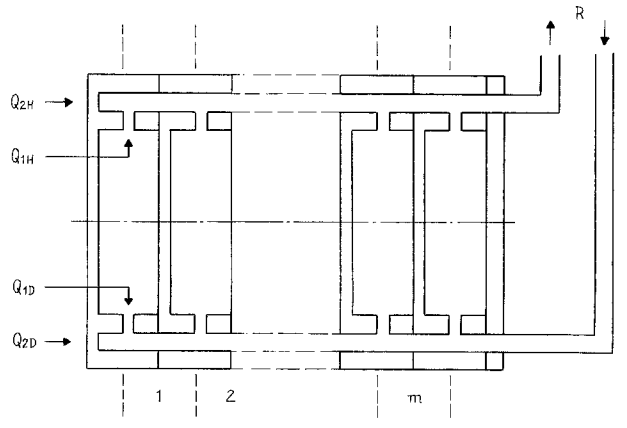

Fig. 3. Scheme of the water electrolyser. Q_{1D} electrolyte inlet; Q_{1H} electrolyte outlet; Q_{2D}, Q_{2H} collecting channels; R to electrolyte reservoir; 1, 2, ... m sections with fictitious bipolar electrodes consisting of short-circuited pairs of cathodes and anodes.

and the equations for the mth (i.e. final) section with the lateral electrolyte channel can be written as

$$A_c + B_c I_{5m-4} - I_{5m-6} R_{1D} - I_{5m-3} R_{2D} - I_{5m-1} R_{1D} = 0 \quad (8)$$

$$A_c + B_c I_{5m-4} - I_{5m-5} R_{1H} - I_{5m-2} R_{2H} - I_{5m} R_{1H} = 0 \quad (9)$$

$$I_{5m-4} + I_{5m-1} + I_{5m} - I_t = 0 \quad (10)$$

$$I_{5m-1} R_{1D} - I_{5m} R_{1H} + I_{5m+1} R_K = 0 \quad (11)$$

$$I_{5m-2} - I_{5m} - I_{5m-1} = 0 \quad (12)$$

$$I_{5m-3} - I_{5m-1} + I_{5m+1} = 0 \quad (13)$$

The total number of equations (and unknowns, I_i) is equal to $5m + 1$. It is convenient to introduce the following dimensionless parameters:

$$A_1 = A_c/I_t R_{1D}, \quad A_2 = A_c/I_t R_{1H} \quad (14)$$

$$B_1 = R_{2D}/R_{1D}, \quad B_2 = R_{2H}/R_{1H}, \quad B_3 = R_K/R_{1H} \quad (15)$$

$$C_1 = B_c/R_{1D}, \quad C_2 = B_c/R_{1H} \quad (16)$$

and the dimensionless currents $X_i = I_i/I_t$.

The above system of equations was put into matrix form and solved by the Gauss elimination method. The simplification of the equivalent circuit, recommended by some authors [19,20], was not used since it was desired to take the asymmetry of the system into account. The values of the input parameters, Equations 14–16, were calculated from the dimensions of the channels and from the tabulated conductivity of KOH solutions (for details see [21]). For 3.5 M KOH, the following equation can be used:

$$\log \kappa = 1.591 - 554.1/T \quad (17)$$

hence $\kappa = 0.751\,\Omega^{-1}\,\mathrm{cm}^{-1}$ at 50 °C, the typical operating temperature. The values of A_c and B_c were determined approximately by measuring the terminal voltage of the electrolyser, U_t, as function of the total

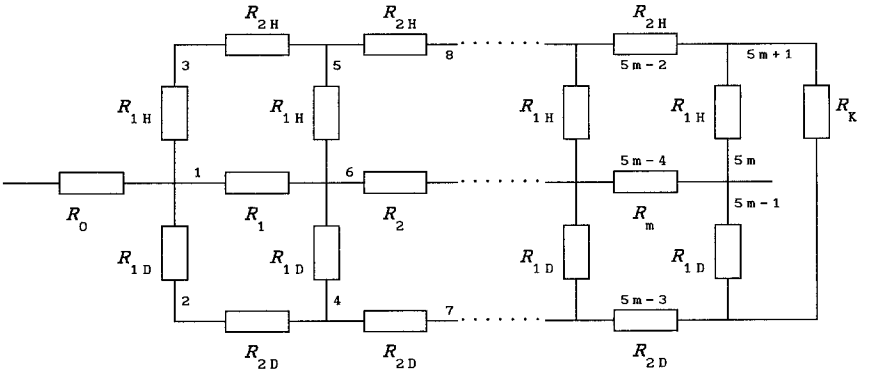

Fig. 4. Equivalent circuit of the water electrolyser. R_0, R_1 through R_m denote resistances of fictitious cells (R_0 corresponds to the first electrode combined with the last one, R_1 through R_m to sections 1 to m in Fig. 3). R_{1H}, R_{2H}, R_{1D} and R_{2D} denote resistances of the channel sections Q_{1H} . . . Q_{2D} in Fig. 3, R_K is the resistance of the lateral channel. The branches are numbered as indicated.

current, I_t. The mean cell voltage is then equal to $U_t/N = U_t/(m + 1)$ and this was expressed by linear regression as $U_t/N = A_c + B_c I_t$. Thus, for a five-cell electrolyser for $I = 1 - 6A$

$$U_t/N = 1.633 + 0.0809 I_t(\mathrm{V}) \text{ at } 45\,^\circ\mathrm{C}, \quad (18a)$$

$$U_t/N = 1.765 + 0.07722 I_t(\mathrm{V}) \text{ at } 22\,^\circ\mathrm{C}. \quad (18b)$$

When the measurements were repeated with another five-cell electrolyser, the results were $A_c = 1.636\,\mathrm{V}$, $B_c = 0.09066\,\Omega$ at 40–45 °C, i.e. nearly the same.

An important measurable quantity is the current efficiency of the electrolyser, given by the equation

$$\eta_I = \frac{1}{N}\left(1 + \frac{1}{I_t}\sum_{i=1}^{N-1} I_{5i-4}\right) \quad (19)$$

With decreasing parasitic currents, the value of η_I approaches unity.

An approximate expression for the cell voltage (which is not involved in the above equations) can be obtained in view of the fact that the hydrogen electrode can be considered practically as nonpolarizable. Then, the voltage of the ith cell is approximately

$$U_i \approx A_c + B_c I_{ai} \quad (20)$$

where I_{ai} denotes the current flowing through the anode (oxygen electrode) of ith cell. It can be seen from Figs 3 and 4 (where the final electrode on the right is an anode) that $I_{a1} = I_1, I_{a2} = I_6, \ldots I_{aN} = I_t$. If Equation 20 is summed over $i = 1$ to N, we obtain the approximate equation

$$\sum_{i=1}^{N} U_i = U_t \approx N(A_c + B_c I_t \eta_I) \quad (21)$$

which can be used to check the correctness of the above considerations.

4. Results and discussion

Calculations of the current efficiency and parasitic currents were performed for more than fifty variants including 5 to 20 cells, total current $I_t = 1 - 5\,A$, and various channel diameters. The results were only slightly influenced by the resistance of the lateral connecting channel, R_K (Fig. 4), but the normalized parasitic currents $X_i = I_i/I_t$ increased with decreasing total current, I_t, and with increasing number of cells, N. This was manifested by corresponding changes of the current efficiency, η_I, determined from the volume of evolved hydrogen.

The following parameters were kept constant (cf. Fig. 3):

Lengths of channels Q_{1H} and Q_{1D}: 12 mm per cell
Length of channel Q_{1H}: 9 mm
Length of channel Q_{1D}: 8 mm
Length of lateral channel: 100 mm
Inner diameter of lateral channel: 5.5 mm

Representative results are summarized in Table 1. The experimental (exp.) values of efficiency, given in the extreme right column, are in good agreement with the theoretical ones. The first two lines refer to the original design of the electrolyser, whereas lines 15–23 refer to the new, improved design. The enlargement of the channel diameters did not cause an appreciable decrease in current efficiency, especially at total currents higher than 1 A, while the electrolyte recirculation improved. This is important since the system must be cooled (through the electrolyte reservoir) and, at the same time, the oxygen evolved must escape in the form of a gas emulsion through channels Q_{1H} and Q_{2H} and through the electrolyte reservoir into the atmosphere.

Figure 5 shows the distribution of normalized parasitic currents in the upper (X_3, X_5, X_{10}, . . . X_{95}) and lower branches (X_2, X_4, X_9, . . . X_{94}) for the parameter values given in the last row of Table 1. The small difference between the first (X_2, X_3) and the last currents (X_{94}, X_{95}) is caused by the lateral channel with resistance R_K; the asymmetry with respect to the axis $X_i = 0$ is due to the difference between the diameters d_{1H} and d_{1D}. The last currents (X_{94}, X_{95}) were inverted in sign to save space.

The values of η_I increase somewhat with decreasing temperature (cf. rows 9–12 in Table 1); this is, however, difficult to observe experimentally owing to the heating effect.

Equation 21 was checked by comparing the experimental value of U_t with the calculated one. Thus, for 20 cells at 22 °C we obtained at $I_t = 5\,\mathrm{A}$; $U_{t,\mathrm{exp}} = 42.86\,\mathrm{V}$, $U_{t,\mathrm{cal}} = 42.27\,\mathrm{V}$; and at $I_t = 1\,\mathrm{A}$: $U_{t,\mathrm{exp}} =$

Table 1. Current efficiency values calculated for different channel diameters and total currents at 45–50 °C. Diameters d_{1H}, d_{2H}, d_{1D} and d_{2D} (in cm) correspond to the channels with the same subscripts in Fig. 3

No.	*N*	I_t/A	d_{1H}	d_{2H}	d_{1D}	d_{2D}	η_i	*Note*
1	5	5	0.2	0.3	0.1	0.3	0.9872	exp. 0.983
2	10	5	0.2	0.3	0.1	0.3	0.9775	
3	5	5	0.3	0.3	0.1	0.3	0.9844	
4	5	1	0.3	0.3	0.1	0.3	0.9343	
5	5	1	0.3	0.1	0.1	0.3	0.9713	Q_{2H} clogged
6	10	5	0.3	0.3	0.1	0.3	0.9757	
7	10	1	0.3	0.3	0.1	0.3	0.8977	
8	20	5	0.3	0.3	0.1	0.3	0.9701	
9	20	5	0.3	0.43	0.1	0.43	0.9437	
10	20	5	0.3	0.43	0.1	0.43	0.9602	at 22 °C
11	20	1	0.3	0.43	0.1	0.43	0.7630	
12	20	1	0.3	0.43	0.1	0.43	0.8296	at 22 °C
13	20	1	0.3	0.43	0.2	0.43	0.7411	
14	20	5	0.3	0.43	0.2	0.43	0.9384	
15	20	1	0.3	0.43	0.3	0.43	0.7329	
16	20	5	0.3	0.43	0.3	0.43	0.9365	
17	5	5	0.35	0.35	0.2	0.35	0.9746	exp. 0.970
18	5	4	0.35	0.35	0.2	0.35	0.9695	exp. 0.970
19	5	3	0.35	0.35	0.2	0.35	0.9610	exp. 0.965
20	5	2	0.35	0.35	0.2	0.35	0.9440	exp. 0.952
21	5	1	0.35	0.35	0.2	0.35	0.8931	exp. 0.919
22	10	5	0.35	0.35	0.2	0.35	0.9634	
23	10	1	0.35	0.35	0.2	0.35	0.8462	
24	20	5	0.35	0.35	0.2	0.35	0.9574	
25	20	1	0.35	0.35	0.2	0.35	0.8209	

36.58 V, $U_{t,cal}$ = 36.58 V, i.e. the same value (other parameters are given in Table 1, rows 10 and 12).

The fact that only the positive (Ni sheet) electrodes of the electrolyser are polarizable brings about a safety feature. When the current drops to any value, or during idling on open circuit, no oxygen appears in the hydrogen evolved at the negative electrodes.

The theory of parasitic currents based on the equivalent circuit shown in Fig. 4 is applicable to the electrolyser type described and permits electrochemical engineering problems to be solved.

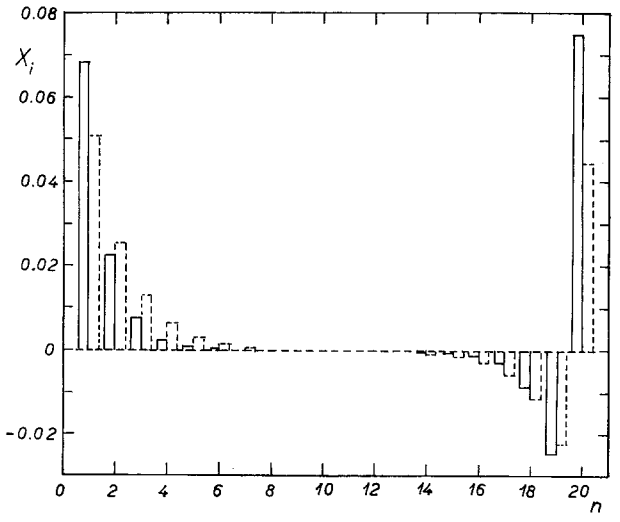

Fig. 5. Distribution of normalized parasitic currents, X_i, in a 20-cell water electrolyser. The last two values were inverted in sign to save space. Solid lines correspond to the upper branches in Fig. 4, dashed lines to the lower branches; *n* denotes the cell number.

References

[1] E. Killer (BBC A.-G. Brown, Boveri & Cie.), *Swiss patent CH655615* (Cl. H01 M8/10), 1986; *Chem. Abstr.* **105** (1986) 50829j.

[2] S. G. Ogryzko-Zhukovskaya, G. P. Belyakov, Yu. I. Golovkin, A. I. Pankratov and Yu. E. Borodkin, *USSR SU 1435664* (Cl. C25 B1/12), 1988; *Chem. Abstr.* **110** (1989) 65732z.

[3] L. Szapert and A. Waszkiewicz, *Polish patent PL 144169* (Cl. C01 B3/02), 1988; *Chem. Abstr.* **111** (1989) 9718h.

[4] M. Nagai (Mitsubishi Heavy Industries, Ltd.), *Jpn Kokai Tokkyo Koho JP 01247591* [89, 247, 591] (Cl. C25 D1/12), 1989; *Chem. Abstr.* **112** (1990) 107353a.

[5] Yi Baolian and Li Guangya, *Sepu* **5** (1987) 332; *Chem. Abstr.* **108** (1988) 78078z.

[6] P. Ragunathan, S. K. Mitra, M. G. Nayar and M. P. S. Ramani, *Trans. SAEST* **20** (1985) 207; *Chem. Abstr.* **104** (1986) 215209b.

[7] J. Divišek, P. Malinowski, J. Mergel and H. Schmiba, *DECHEMA-Monogr.* **98** (1985) (Tech. Elektrolysen) 389; *Chem. Abstr.* **104** (1986) 77646p.

[8] W. Huq, J. Divišek, J. Mergel, W. Seeger and H. Steeb, *Adv. Hydrogen Energy* **8** (1990) (Hydrogen Energy Prog. 8, Vol. 2) 681; *Chem. Abstr.* **115** (1991) 169002f.

[9] H. Vandenborre, R. Leysen, H. Nackaerts, D. van der Eecken, P. van Asbroeck, W. Smets and J. Piepers, *Adv. Hydrogen Energy* **4** (1984) (Hydrogen Energy Prog. 5, Vol. 2) 703; *Chem. Abstr.* **102** (1985) 14079u.

[10] E. W. Justi and A. W. Winsel, Kalte Verbrennung. F. Steiner, Wiesbaden (1962).

[11] H. H. Ewe, E. W. Justi and A. W. Kalberlah, *Energy Conversion* **11** (1971) 149.

[12] J. Jansta and O. Lasota, *Czech. Patent AO 160786* (1971).

[13] O. Lasota, *Chem. Listy* **73** (1979) 974.

[14] F. P. Dousek and O. Lasota, *Nauchn. Appar. (Warszaw)* **4** (1989) 53.

[15] F. P. Dousek, J. Jansta and J. Říha, *Czech. Patent 115599* (1963).

[16] F. P. Dousek, J. Jansta and J. Říha, *Collect. Czech. Chem. Commun.* **31** (1966) 457.

[17] F. P. Dousek and J. Jansta, *Powder Technol.* **4** (1970/71) 83.

[18] I. Roušar and V. Cezner, *J. Electrochem. Soc.* **121** (1974) 648.

[19] I. Roušar, K. Micka and A. Kimla, 'Electrochemical Engineering', Vol. I, Elsevier, Amsterdam (1986).
[20] R. E. White, C. W. Walton, H. S. Burney and R. N. Beaver, *J. Electrochem. Soc.* **133** (1986) 485.
[21] K. Micka and I. Roušar, *Collect. Czech. Chem. Commun.* **34** (1969) 3197.